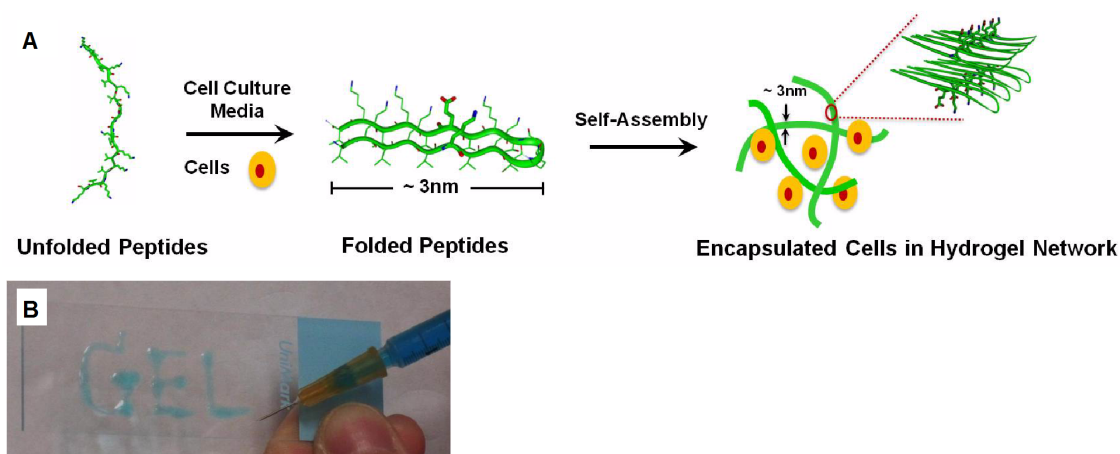


## **Iterative design of peptide-based hydrogels and the effect of network electrostatics on primary chondrocyte behavior**

Chomdao Sinthuvanich, Lisa A. Haines-Butterick, Katelyn J. Nagy and Joel P. Schneider

### **Supporting Information Table of Contents**

<b>Page</b>	<b>Content</b>
2	Figure S1. (A) Triggered peptide folding and self-assembly scheme. (B) Shear-thin/recovery syringe delivery of gel
3	Energy Minimization of HIT2 and HLT2 Electron Microscopy Analysis of MAX8 and HLT2
4	Figure S2. Molecular models of HIT2 and HLT2
5	Figure S3. Transmission electron microscopy of MAX8 and HLT2
6	Figure S4. (A) Analytical RP-HPLC chromatogram of purified MAX8, (B) ESI (+) mass spectrum of purified MAX8
7	Figure S5. (A) Analytical RP-HPLC chromatogram of purified HE1 (B) ESI (+) mass spectrum of purified HE1
8	Figure S6. Analytical RP-HPLC chromatogram of crude HIT1
9	Figure S7. (A) Analytical RP-HPLC chromatogram of purified HIT2 (B) ESI (+) mass spectrum of purified HIT2
10	Figure S8. (A) Analytical RP-HPLC chromatogram of purified HLT2 (B) ESI (+) mass spectrum of purified HLT2



**Figure S1.** (A) To initially encapsulate cells, unfolded peptides are first dissolved in aqueous buffer of low ionic strength. The subsequent addition of cell culture media triggers peptide folding into a  $\beta$ -hairpin conformation that undergoes rapid self-assembly, forming a fibrillar hydrogel network. When cells are present in the media, they are directly encapsulated in the hydrogel. Salt bridge interactions between lysine and glutamate side chains are shown in stick representation. Cells not drawn to scale. (B) Hydrogels formed directly in a syringe can be shear-thin delivered; a blue dye has been encapsulated to aid visualization.

### **Energy Minimization of HIT2 and HLT2**

Molecular models of both HIT2 and HLT2 were prepared in Discovery Studio 3.1 (Accelrys). Each sequence was pre-organized in a canonical beta-hairpin conformation containing a type II' beta turn. Each peptide was energy minimized employing a CHARMM forcefield and implicit water (dielectric set at 80). A two-step protocol was employed for the minimization. First, all backbone atoms were constrained and the side chain atoms minimized using a steepest decent algorithm. This was followed by an all atom minimization using steepest decent with an RMS gradient tolerance of 3, followed by a conjugate gradient algorithm.

### **Electron Microscopy Analysis of MAX8 and HLT2**

Images of diluted hydrogel samples were obtained using a Hitachi H-7650 transmission electron microscope at a voltage of 80 kV. Hydrogels were prepared the night before each TEM experiment was to occur. For each sample, 1 wt % peptide stock solutions in cold double-distilled water were prepared. To each solution an equal volume of cold 100 mM BTP 300 mM NaCl was added to initiate gelation. After overnight incubation, a small aliquot of the resulting 0.5 wt% gel was removed, diluted 40x with water and mixed well. 2  $\mu$ L of the resulting diluted gel sample was placed onto a 200 mesh carbon coated copper grid and excess sample liquid was blotted away with filter paper. A solution of 1 % uranyl acetate was then added to the grid as a negative stain to enhance contrast between fibrils and the background. Excess stain was blotted away and the grids were imaged immediately.

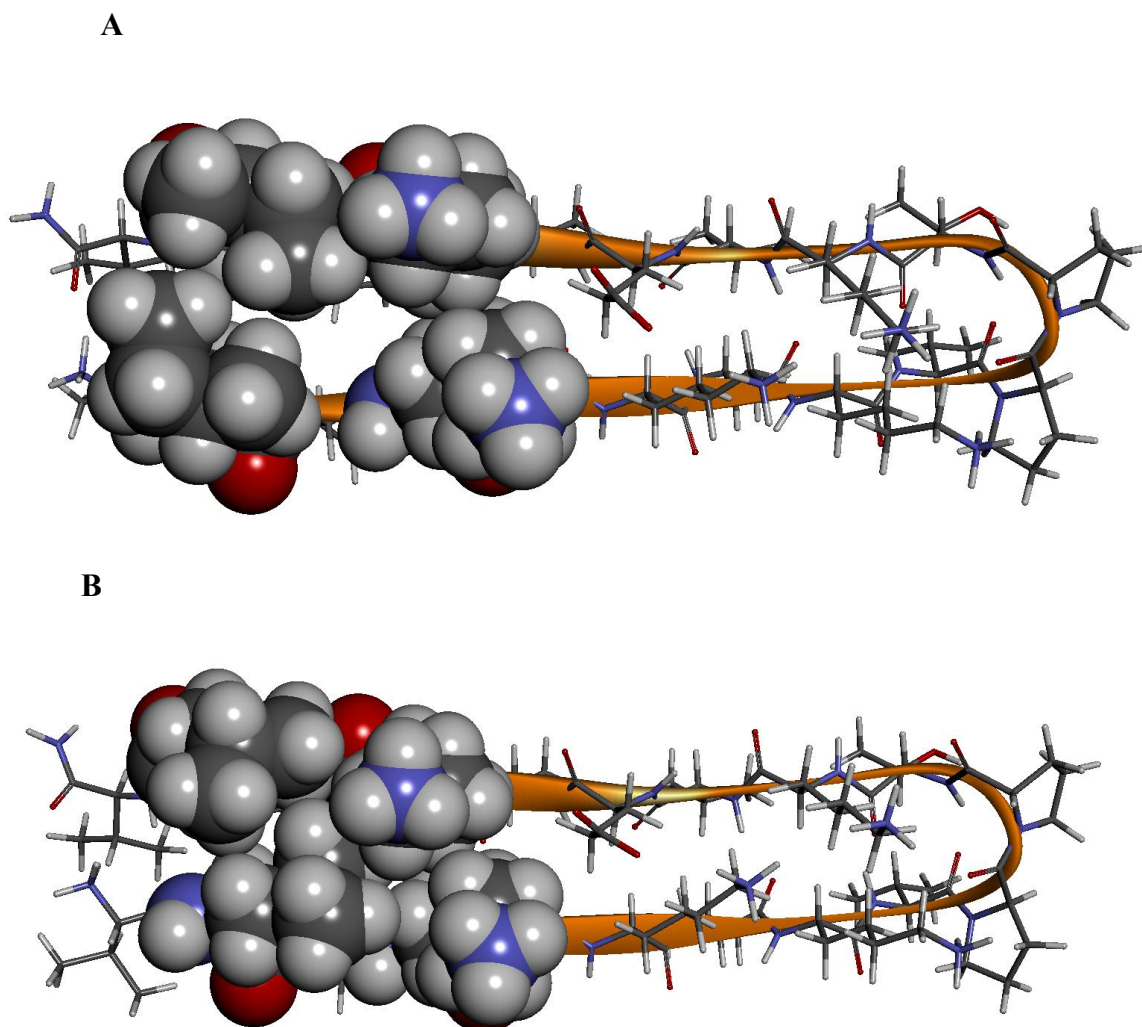


**Figure S1.** Energy minimized structures of HIT2 and HLT2. (A) Nested hydrophobic interaction formed between the two isoleucines at positions 2 and 19 of HIT2 shown in CPK rendering. Also shown are the side chain packing interactions between the isoleucines and the neighboring lysine side chains on the hydrophilic face. (B) Nested hydrophobic interaction formed between the two leucines at positions 2 and 19 of HLT2 shown in CPK rendering. Also shown are the side chain packing interactions between the isoleucines and the neighboring lysine side chains on the hydrophilic face.

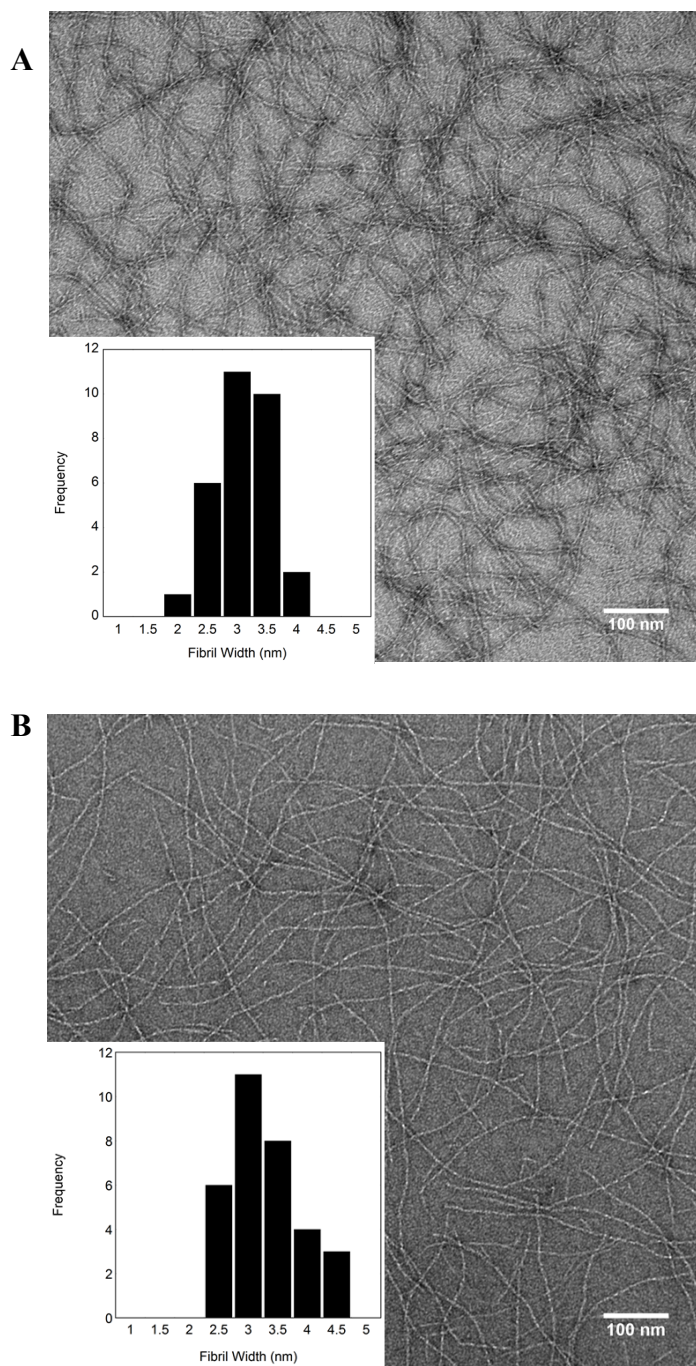


**Figure S2.** Representative transmission electron micrographs of (A) MAX8 and (B) HLT2. The insets show frequency distributions of measured fibril widths from  $n = 30$  independent measurements. Average width for both fibrils is approximately 3 nm.

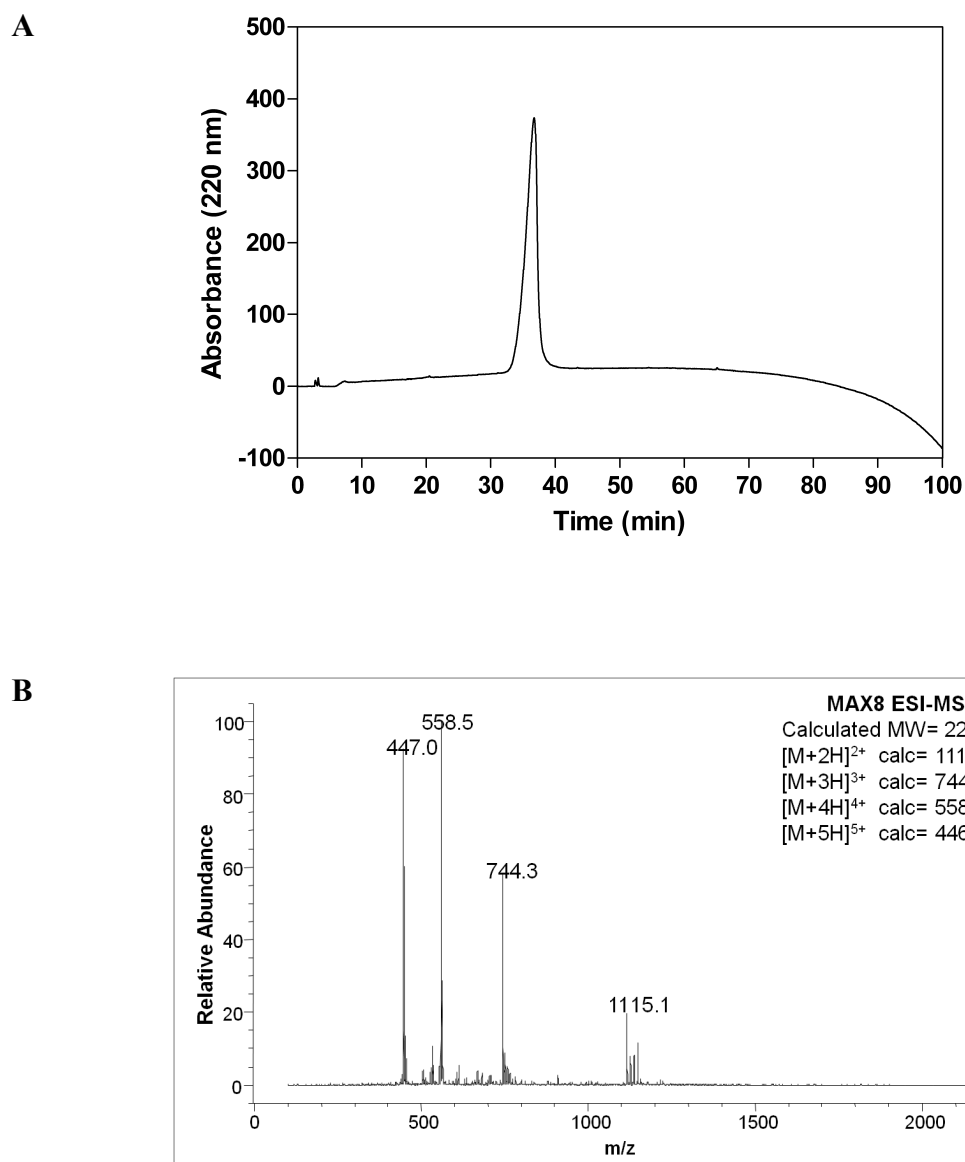


Figure S3. (A) Analytical RP-HPLC chromatogram of purified MAX8 employing Vydac C18 column, 0-100% B in 100 min, (B) ESI (+) mass spectrum of purified MAX8

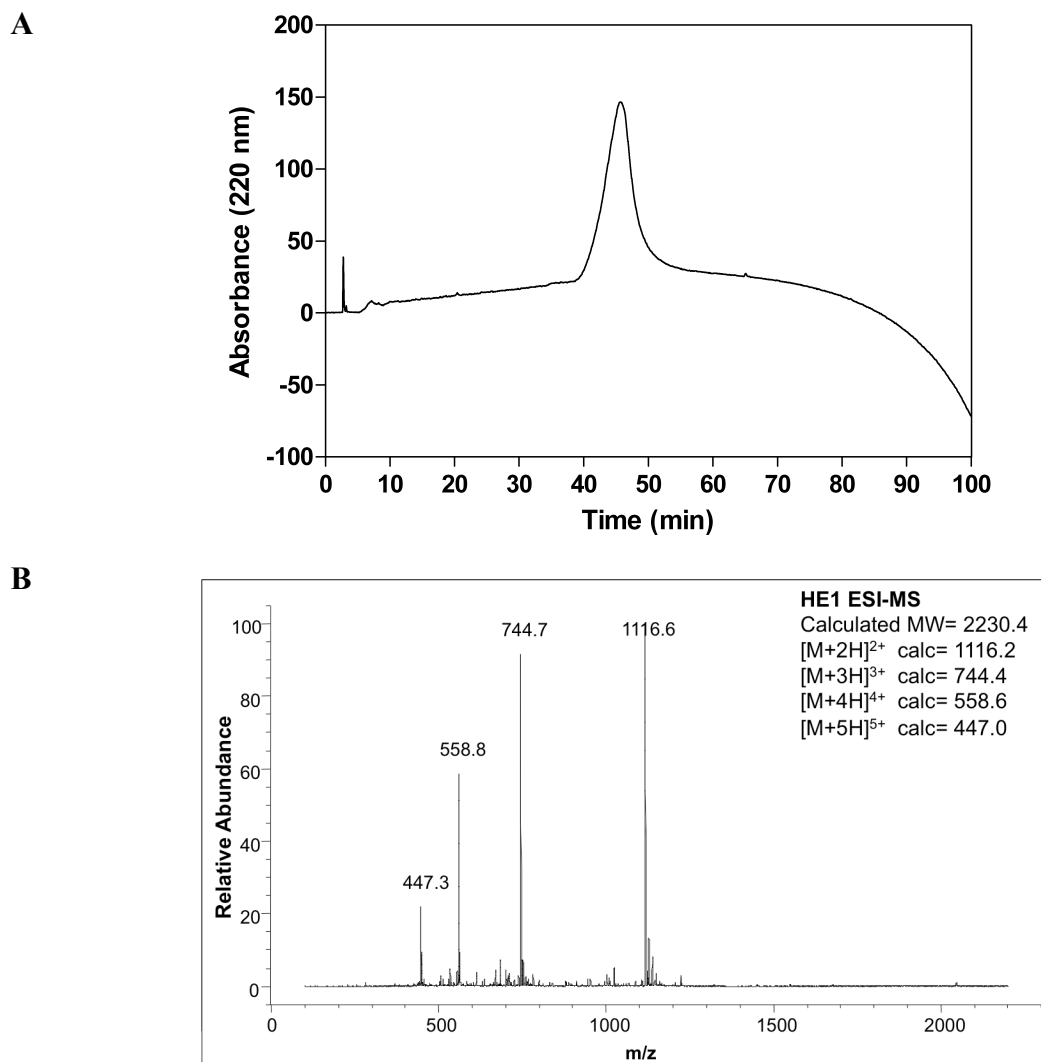


Figure S4. (A) Analytical RP-HPLC chromatogram of purified HE1 employing Vydac C18 column, 0-100% B in 100 min, (B) ESI (+) mass spectrum of purified HE1

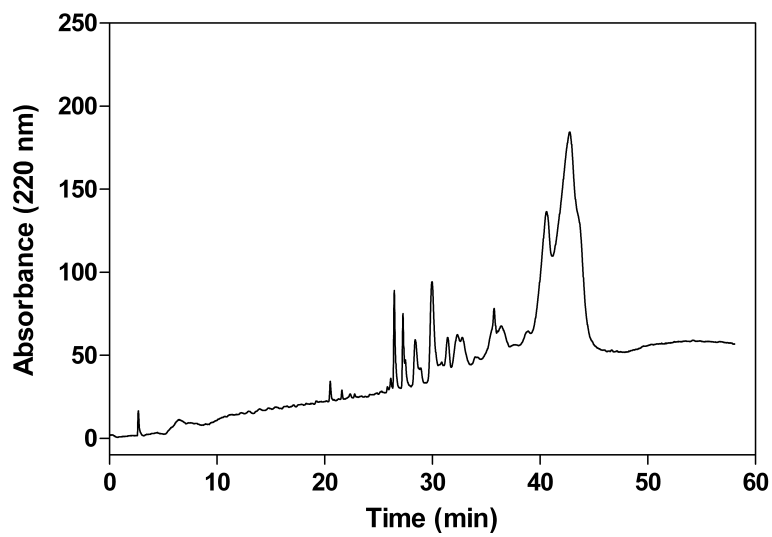
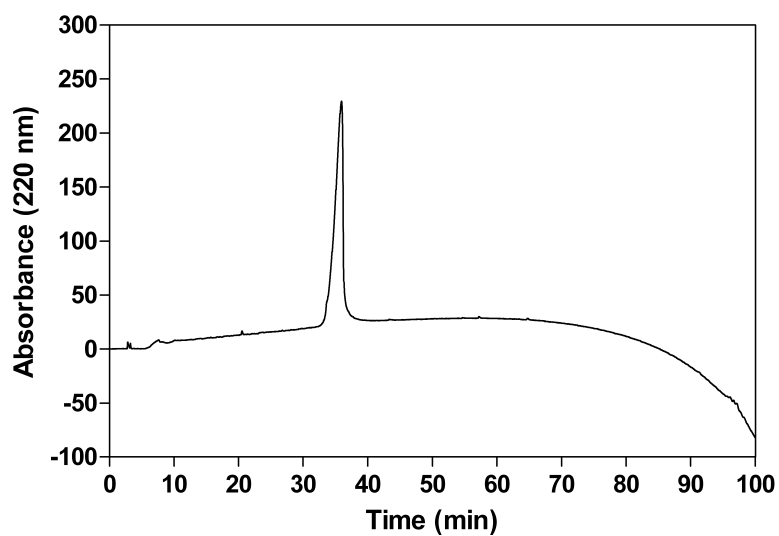


Figure S5. (A) Analytical RP-HPLC chromatogram of crude HIT1 employing Vydac C18 column, 0-60% B in 60 min, (B) ESI (+) mass spectrum of purified HIT1



A



B

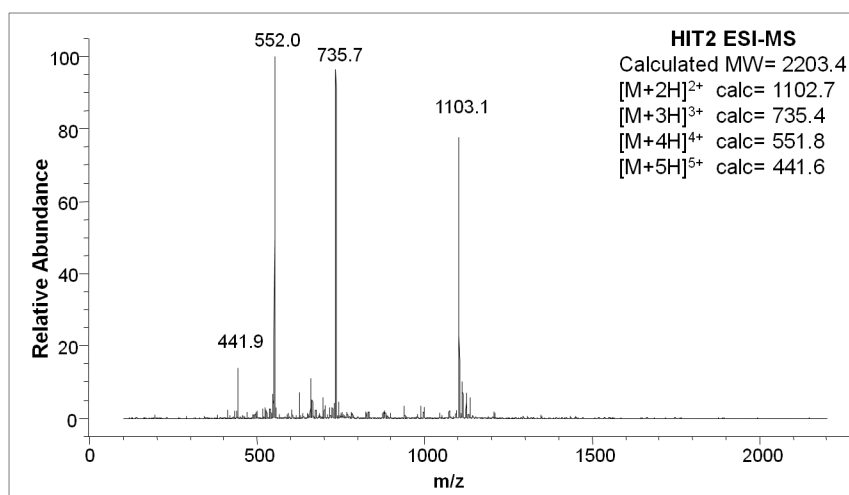


Figure S6. (A) Analytical RP-HPLC chromatogram of purified HIT2 employing Vydac C18 column, 0-100% B in 100 min, (B) ESI (+) mass spectrum of purified HIT2

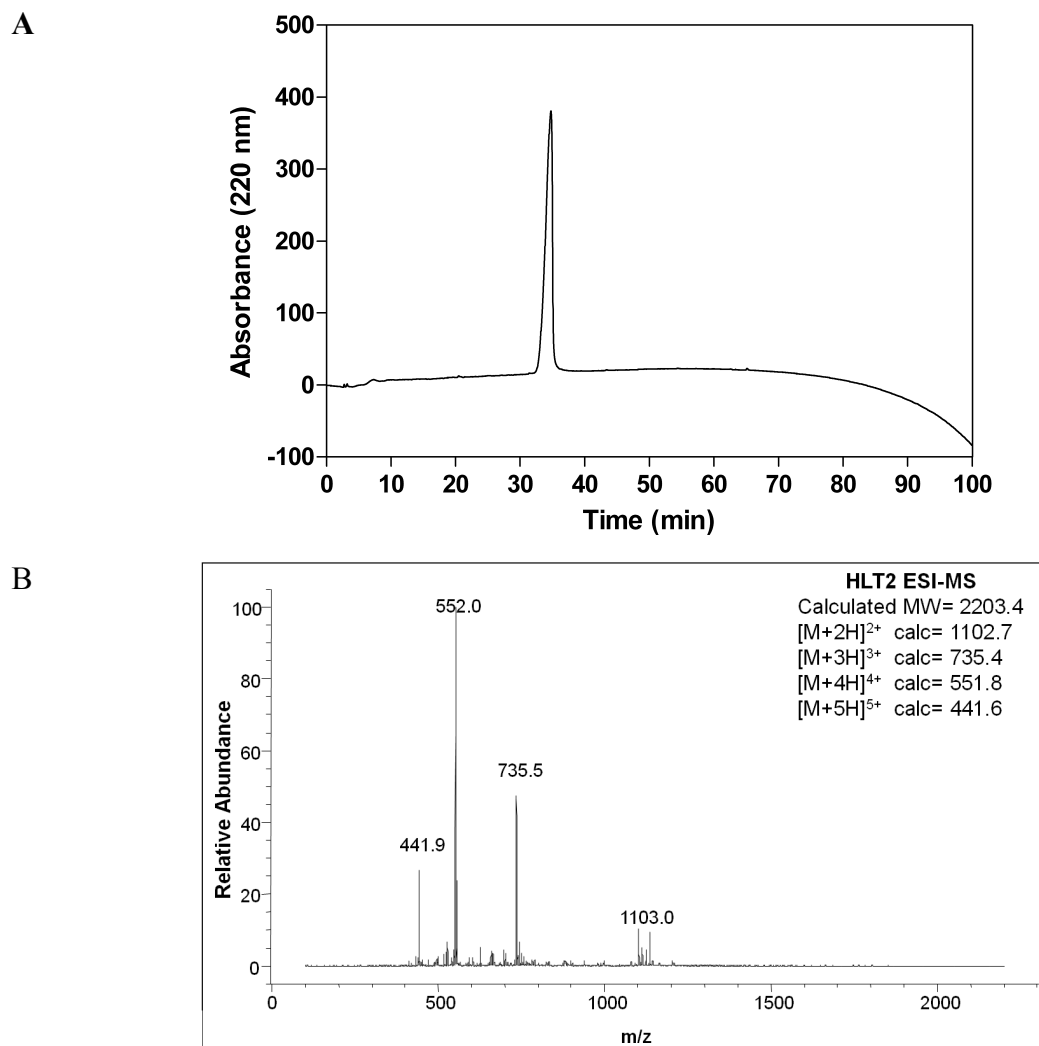


Figure S7. (A) Analytical RP-HPLC chromatogram of purified HLT2 employing Vydac C18 column, 0-100% B in 100 min, (B) ESI (+) mass spectrum of purified HLT2